Journal of Fluorine Chemistry 162 (2014) 9–16

Contents lists available at ScienceDirect

Journal of Fluorine Chemistry

journal homepage: www.elsevier.com/locate/fluor

Fluorine/phenyl chelated boron complexes: Synthesis, fluorescence properties and catalyst for transfer hydrogenation of aromatic ketones

Ahmet Kilic [a,*], Murat Aydemir [b,e], Mustafa Durgun [a], Nermin Meriç [b], Yusuf Selim Ocak [c,e], Armagan Keles [a], Hamdi Temel [d,e]

[a] Department of Chemistry, Faculty of Science, University of Harran, 63190 Şanlıurfa, Turkey
[b] Department of Chemistry, Faculty of Science, University of Dicle, 21280 Diyarbakir, Turkey
[c] Department of Science, Faculty of Education, University of Dicle, 21280 Diyarbakir, Turkey
[d] Department of Pharmaceutical Chemistry, Faculty of Pharmacy, Dicle University, Diyarbakir 21280, Turkey
[e] Science and Technology, Application and Research Center (DUBTAM), Dicle University, Diyarbakir 21280, Turkey

ARTICLE INFO

Article history:
Received 28 January 2014
Received in revised form 3 March 2014
Accepted 8 March 2014
Available online 16 March 2014

Keywords:
Fluorinated boron complexes
Fluorescence
Catalysts
Transfer hydrogenation
Ketone

ABSTRACT

The synthesis of salen/salan ligands ($\mathbf{L_1}$ and $\mathbf{L_2}$) and their fluorine/phenyl chelated boron complexes [$\mathbf{L_{(1,2)}BF_2}$] or [$\mathbf{L_{(1,2)}BPh_2}$] is described in this paper. The fluorine/phenyl chelated boron complexes were synthesized from the reaction of $BF_3{\cdot}OEt_2$ or BPh_3 with the corresponding ligands in different solvent. The boron complexes display high stability and can be handled in air due to the presence of coordinative B ← N and covalent B–O bonds in their structures. The salen/salan ligands (designated as salan, a saturated version of the corresponding salen ligands) and their fluorine/phenyl chelated boron complexes have been characterized by ^1H, ^{13}C NMR and ^{19}F NMR spectra, elemental analysis, FT-IR spectra, UV–vis spectra, LC–MS spectra, melting point and fluorescence spectroscopy. The fluorescence efficiencies of BF_2–chelate boron complexes are greatly improved compared to those of the BPh_2–chelate boron analogs based on the same salen/salan ligands, probably due to the enhanced conjugation degree of the diphenyl boron chelation, which can effectively prevent molecular aggregation. The boron complexes [$\mathbf{L_{(1,2)}BF_2}$] or [$\mathbf{L_{(1,2)}BPh_2}$] were also applied to the transfer hydrogenation of aromatic ketones to the corresponding alcohol derivatives in the presence of *iso*-PrOH as the hydrogen source. Catalytic studies showed that all complexes are good catalytic precursors for transfer hydrogenation of aryl alkyl ketones in 0.1 M *iso*-PrOH solution. This transfer hydrogenation is characterized by low reversibility under these conditions.

1. Introduction

The fluorine/phenyl chelated boron complexes, one of the most important types of fluorescent dyes, have been extensively studied. In recent years, fluorescent materials of organic fluorine or phenyl boron complexes continue to be developed because of their utilities in many various fields of current research, and the many important applications in science and technology. Among boron compounds, as the most well-known and having excellent fluorescent properties is borondipyrromethenes (BODIPYs) with *N*,*N*-bidentate ligands [1–8]. These types of compounds are widely used as chemosensors [9,10], organic light-emitting diodes (OLEDs) [11,12], electron-transport materials [13,14], sensitizers in solar cells [15,16], nonlinear optics [17,18] as well as antibacterial properties [19] and hydrogen-transfer catalysts [20–22]. Therefore, in recent years, design and synthesis of novel boron compounds to explore their broad applications have attracted much attention. Among boron compounds, three main types of BF_2/BPh_2 chelated boron complexes are classified as *N*,*N*-bidentate, *N*,*O*-bidentate and *O*,*O*-bidentate compounds. Compared with three-coordinated boron complexes, which require bulky substituents (such as mesityl or other groups) to stabilize four-coordinated boron complexes are in general stable and can be obtained readily [23]. Also, it is known that boron is strongly electrophilic by virtue of its tendency to fill the vacant orbital and complete the octet, so in contrast to organometallic compounds, organoboron compounds are in general more stable due to the increased covalency of B–O and B ← N bonds [24]

* Corresponding author at: Department of Chemistry, Harran University, TR-63190 Şanliurfa, Turkey. Tel.: +90 4143183587; fax: +90 4143183541.
E-mail address: kilica63@harran.edu.tr (A. Kilic).

http://dx.doi.org/10.1016/j.jfluchem.2014.03.004
0022-1139/

Catalytic transfer hydrogenation is an effective method for the reduction of ketones and aldehydes to alcohols under mild reaction conditions [25–27]. Transfer hydrogenation with the aid of a stable hydrogen donor is a useful alternative method for catalytic hydrogenation by molecular hydrogen [28,29]. In transfer hydrogenation, organic molecules such as primary and secondary alcohols [30] or formic acid and its salts [31] have been employed as the hydrogen source. The use of the hydrogen donor has some advantages over the use of molecular hydrogen since it avoids risks and constraint associated with hydrogen gas as well as the necessity for pressure vessels and other equipments. A number of transition metal complexes are known to be catalyzing hydrogen transfer from an alcohol to a ketone [32]. In the mid 1920s, Meerwein, Verley and Ponndorf (MPV-reaction), respectively, reported the first examples of hydrogen transfer from an alcohol to a ketone [33–35]. The first example of a transition metal-catalyzed transfer hydrogenation, employing an Ir-DMSO-complex, was presented in 1967 by Trocha-Grimshaw and Henbest [36]. Recently, Ikariya and coworkers have reviewed bifunctional transition metal-based molecular catalysts for transfer hydrogenation of ketones under different experimental conditions [37].

Some catalyst systems are expensive because synthesis of compounds requires many chemical synthetic steps. Hence, there is a need for economic, relatively mild and environmentally friendly catalyst system. So, we preferred the BF_2/BPh_2 chelated boron complexes as catalyst for transfer hydrogenation of aromatic ketones. As far as we know, there are few reports on BF_2/BPh_2 chelated boron complexes containing salen/salan ligands have been used as catalysts for transfer hydrogenation of aromatic ketones. Compounds of this type are considerably interesting for their simple synthesis, easily accessibility and good luminescence and fluorescence properties. Interestingly, a few of *N*,*O*-bidentate BF_2/BPh_2 chelated boron compounds are the efficient hydrogen-transfer catalysts. In this work, salen/salan ligands were selected because they can function as chelating ligands upon treatment with a boron compounds such as BPh_3 or $BF_3{\cdot}OEt_2$ conjugated π-systems that was good for studying the catalytic transfer hydrogenation of aromatic ketones. As a continuation of our previously reported work, we have synthesized BF_2/BPh_2 chelated boron complexes containing electron withdrawing or electron-donating substituents on their ligands. We show that salen/salan ligands (**L_1** and **L_2**) and their boron complexes [**$L_{(1,2)}BF_2$**] or [**$L_{(1,2)}BPh_2$**] display attractive fluorescence and catalytic activity.

2. Results and discussion

2.1. Synthesis of compounds

As summarized in Scheme 1, the salen ligand (**L_1**) was prepared in moderate yield by refluxing the 1:1 molar ratio of 3,5-di-*tert*-butylsalicylaldehyde and 4-amino-2,2,6,6-tetramethylpiperidine in absolute ethanol and in the presence of 3-4 drops of formic acide as catalyst. The salan ligand (**L_2**) has been prepared by reduction of the corresponding salen ligand (**L_1**) with $NaBH_4$ and in EtOH solution. Both salen ligand (**L_1**) and salan ligand (**L_2**) are obtained in good yield, 86 and 78%, respectively, as yellow or white solid. The satisfactory spectroscopic results were acquired for both salen ligand (**L_1**) and salan ligand (**L_2**). As anticipated, treatment of the salen ligand (**L_1**) or salan ligand (**L_2**), with an excess of boron reagent $BF_3.OEt_2$ in anhydrous benzene and in the presence of Et_3N or with an excess of boron reagent BPh_3 in anhydrous toluene under N_2 atmosphere afforded the boron complexes [**$L_{(1,2)}BF_2$**] or [**$L_{(1,2)}BPh_2$**], respectively as outlined in Scheme 2. Both BF_2-chelated boron complexes [**$L_{(1,2)}BF_2$**] and BPh_2-chelated ones [**$L_{(1,2)}BPh_2$**] are obtained in good yield (72–65%) as yellow or white solids after purification by column chromatography. Again, the satisfactory spectroscopic results were acquired for all boron complexes. We chose to employ the the salen ligand (**L_1**) and salan ligand (**L_2**) and their boron complexes [**$L_{(1,2)}BF_2$**] or [**$L_{(1,2)}BPh_2$**] for several reasons: they are (1) easily prepared, (2) scarcely seen in literature, (3) to the best of our knowledge, there are few reports that boron complexes containing the salen/salan ligands used as catalyst for the transfer hydrogenation of aromatic and (4) the salen/salan ligands bind strongly to boron ions. The salen ligand (**L_1**) and salan ligand (**L_2**) and their boron complexes [**$L_{(1,2)}BF_2$**] or [**$L_{(1,2)}BPh_2$**] are stable in different solutions and in the solid state upon extended exposure to air. This high chemical stability in this class of compounds is attributed to the bidentate chelation of the salen ligand (**L_1**) and salan ligand (**L_2**) to the boron center. Although much effort was made to obtain single crystals of the compounds, we failed to do so. However, the ^1H, ^{13}C NMR and ^{19}F NMR spectra, elemental analysis, FT-IR spectra, UV–vis spectra, LC–MS spectra, melting points and fluorescence spectra support to the proposed structures.

2.2. Spectroscopic characterization

The ^1H and ^{13}C NMR of the salen (**L_1**) and salan (**L_2**) ligands and their fluorine/phenyl boron complexes [**$L_{(1,2)}BF_2$**] and [**$L_{(1,2)}BPh_2$**]

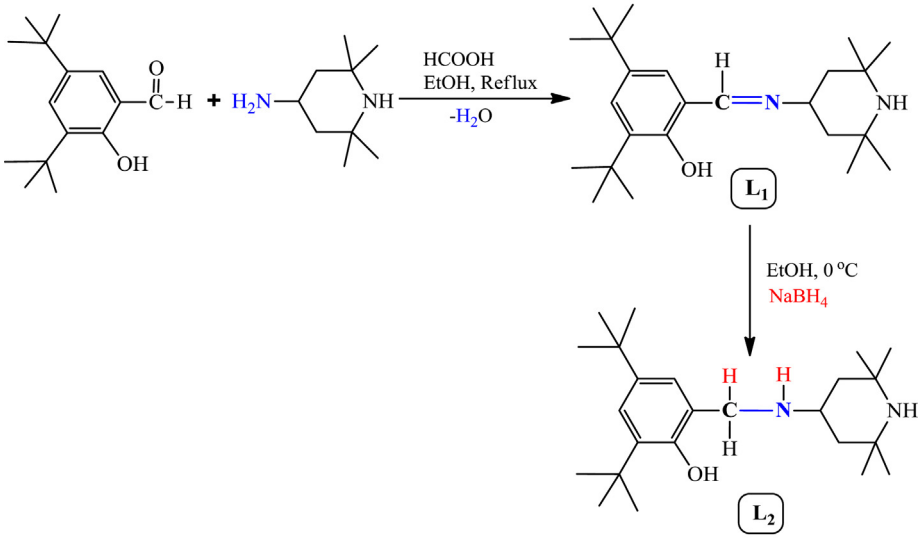

Scheme 1. Synthesis of the salen/salan ligands (**L_1** and **L_2**).

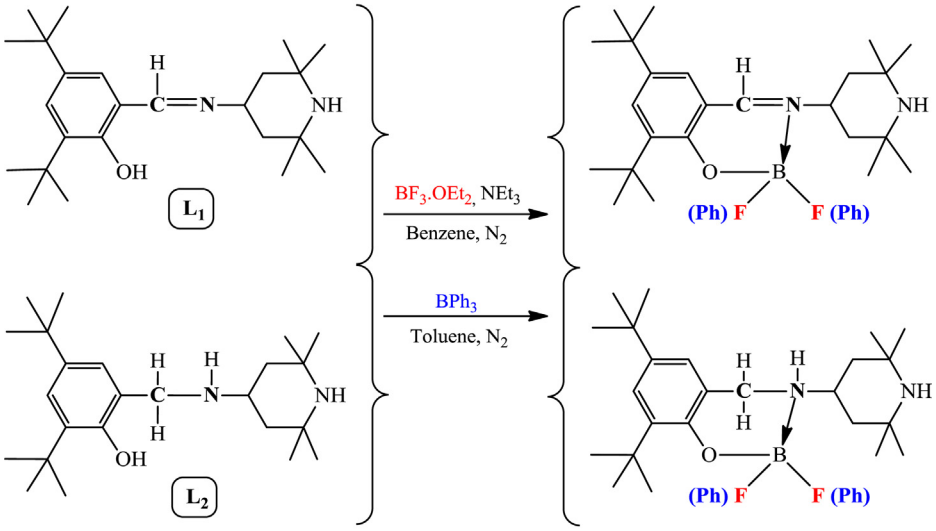

Scheme 2. Synthesis of the [$\mathbf{L_{(1,2)}BF_2}$] and [$\mathbf{L_{(1,2)}BPh_2}$] boron complexes.

have been recorded in $CDCl_3$ at room temperature, and also, the ^{19}F NMR of the fluorinated boron complexes [$\mathbf{L_1BF_2}$] and [$\mathbf{L_2BF_2}$] have been recorded in DMSO-d_6 at room temperature, and the assignments are listed in the experimental section. The disappearance of the signal due to phenolic OH protons (δ = 13.91 ppm for ($\mathbf{L_1}$) and δ = 13.82 ppm for ($\mathbf{L_2}$), which disappear on D_2O addition) in all boron complexes refers to their involvement in coordination with the boron center which implies the formation of B–O bond in these boron complexes, as expected. The resonance for the azomethine –CH=N– proton of salen ligand ($\mathbf{L_1}$) (δ = 8.49 ppm) shifts to highfield in complexes as δ 8.38 ppm in [$\mathbf{L_1BF_2}$] and δ 8.31 ppm in [$\mathbf{L_1BPh_2}$]. Furthermore, in the ^{13}C NMR spectra, the signals for carbon atoms of the same group were observed at δ 164.54, 163.32 and 160.93 ppm for ($\mathbf{L_1}$), [$\mathbf{L_1BF_2}$] and [$\mathbf{L_1BPh_2}$], respectively. The resonances for the azomethine –CH=N proton the ^1H and those of carbon in the ^{13}C NMR spectra shifts to lower field compared to those of free ligand, indicating the formation of B–N bond and also confirming the participation of the iminic nitrogen atoms in coordination for boron complexes [3]. Distinctive signals for salan ligand ($\mathbf{L_2}$) and its boron [$\mathbf{L_2BF_2}$] and [$\mathbf{L_2BPh_2}$] complexes are observed in the range 4.50–4.03 ppm for CH_2–NH proton in their ^1H NMR spectra (see experimental section) and in the range 47.61–46.09 ppm for CH_2–NH carbon in their ^{13}C NMR spectra, as expected. Additionally for [$\mathbf{L_1BF_2}$] and [$\mathbf{L_2BF_2}$] complexes, in the ^{19}F NMR spectrum of each complex, the resonances are found at δ = −148.35 for [$\mathbf{L_1BF_2}$] and δ = −148.44 ppm for [$\mathbf{L_1BF_2}$] as quartet signal, respectively. These resonances show that another solid evidence for the chelation of the BF_2 group with the salen ($\mathbf{L_1}$) and salan ($\mathbf{L_2}$) ligands. These values and the other NMR data are in good agreement with the proposed structures.

The main FT-IR frequencies of the salen ($\mathbf{L_1}$) and salan ($\mathbf{L_2}$) ligands and their fluorine/phenyl boron complexes [$\mathbf{L_{(1,2)}BF_2}$] and [$\mathbf{L_{(1,2)}BPh_2}$] along with their proposed assignments are given in the experimental section. Intermolecular H-bond (O–H···N) gives a band at 3182–2640 cm^{-1} in FT-IR spectra of free salen ($\mathbf{L_1}$) and salan ($\mathbf{L_2}$) ligands, which disappears in those of boron complexes [$\mathbf{L_{(1,2)}BF_2}$] and [$\mathbf{L_{(1,2)}BPh_2}$], indicating deprotonation of organic ligand through coordination. On the other hand, the existence of an υ(B–O) peak in the range 1190–1183 cm^{-1} for the boron complexes, provide conclusive evidence for the formation of foregoing boron complexes [21]. A band was observed at 1632 cm^{-1} in the FT-IR spectra of salen ligand ($\mathbf{L_1}$) distinctive from salan ligand ($\mathbf{L_2}$), owing to azomethine υ(HC=N) group. In the FT-IR spectra of [$\mathbf{L_1BF_2}$] and [$\mathbf{L_1BPh_2}$], this band was observed at ~1620 cm^{-1} showing a small frequency shift [38], which may be attributed to the formation of B ← N dative bond in these complexes. Since salen ligand ($\mathbf{L_1}$) is converted to salan ligand ($\mathbf{L_2}$), this peak is not observed for other boron complexes, as expected. Appearance of the strong stretching vibrations in the region of 1060–1057 cm^{-1} for [$\mathbf{L_{(1,2)}BF_2}$] and in the region of 1028–1017 cm^{-1} for [$\mathbf{L_{(1,2)}BPh_2}$] may be due to the B ← N vibration mode and those in the region of 882–876 cm^{-1} were attributed to the B–F stretching vibrations for [$\mathbf{L_{(1,2)}BF_2}$] complexes and in the region of 886–882 cm^{-1} were attributed to the B–Ph stretching vibrations for [$\mathbf{L_{(1,2)}BPh_2}$] complexes [39,40].

The absorption spectral characteristics of the salen ($\mathbf{L_1}$) and salan ($\mathbf{L_2}$) ligands and their fluorine/phenyl boron [$\mathbf{L_{(1,2)}BF_2}$] and [$\mathbf{L_{(1,2)}BPh_2}$] complexes were studied in CH_3OH or THF solutions at room temperature, in the range 200–1100 nm, and the results are given in the experimental section. To make a reliable comparison, the UV–vis absorption spectral behaviors of the salen ($\mathbf{L_1}$) and salan ($\mathbf{L_2}$) ligands and their fluorine/phenyl boron [$\mathbf{L_{(1,2)}BF_2}$] and [$\mathbf{L_{(1,2)}BPh_2}$] complexes were studied under the same experimental conditions. Upon complexation with boron ions, new absorption bands appearing at 220–402 nm in CH_3OH and 226–398 nm in THF were attributed to $\pi \rightarrow \pi^*$ or $n \rightarrow \pi^*$, while charge transfer (CT) transitions were found to be shifted to lower or higher energy regions compared to the those of free ligands. Furthermore, appearance of new bands at longer wavelength may be assigned to ligand to boron center charge transfer (LBCT) transitions. The characteristic absorption bands below 292 nm in CH_3OH or THF solutions are practically identical and can be attributed to $\pi \rightarrow \pi^*$ transitions in the phenyl ring or azomethine (–CH=N–) groups. The other absorption bands observed within the range of 328–352 nm in CH_3OH or THF solutions are most probably due to $n \rightarrow \pi^*$ transition of azomethine (–CH=N–) moiety. In the lower-energy region, the absorption spectra show new bands at 391–402 nm in CH_3OH or THF solutions are most probably assigned as charge-transfer transitions.

The fluorescence data of the salen ($\mathbf{L_1}$) and salan ($\mathbf{L_2}$) ligands and their fluorine/phenyl boron [$\mathbf{L_{(1,2)}BF_2}$] and [$\mathbf{L_{(1,2)}BPh_2}$] complexes were studied in THF solvent and the results are given in Figs. 1–3. As shown in Fig. 1, the salen ($\mathbf{L_1}$) and salan ($\mathbf{L_2}$) ligands exhibit fluorescence emission band located at 388 nm when excited at 354 nm for ($\mathbf{L_1}$), the emission band is located 385 nm when excited at 340 nm for ($\mathbf{L_2}$), which can be assigned to $\pi \rightarrow \pi^*$ transition [41]. The emission spectra shift to longer wavelengths due to the existence azomethine (–CH=N–) group in the salen ($\mathbf{L_1}$) ligand or

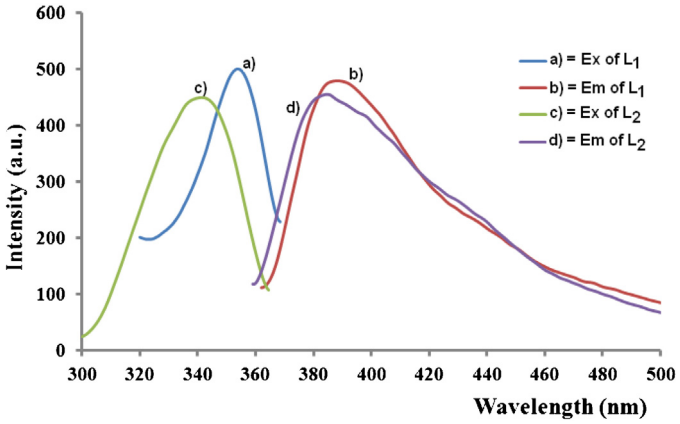

Fig. 1. The fluorescence spectra of salen/salan ligands ($\mathbf{L_1}$ and $\mathbf{L_2}$) recorded in THF.

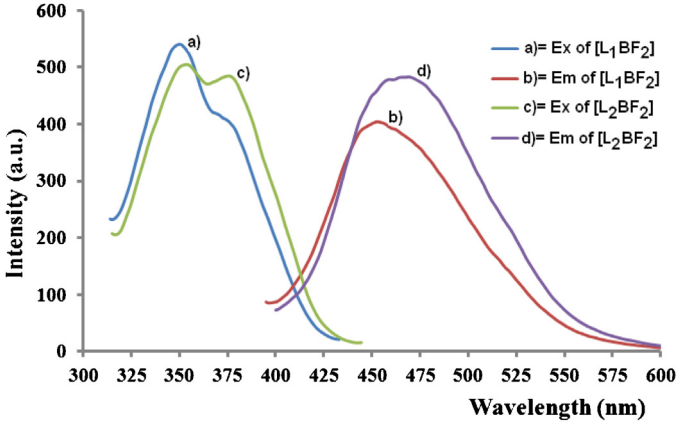

Fig. 2. The fluorescence spectra of $[\mathbf{L_{(1,2)}BF_2}]$ boron complexes recorded in THF.

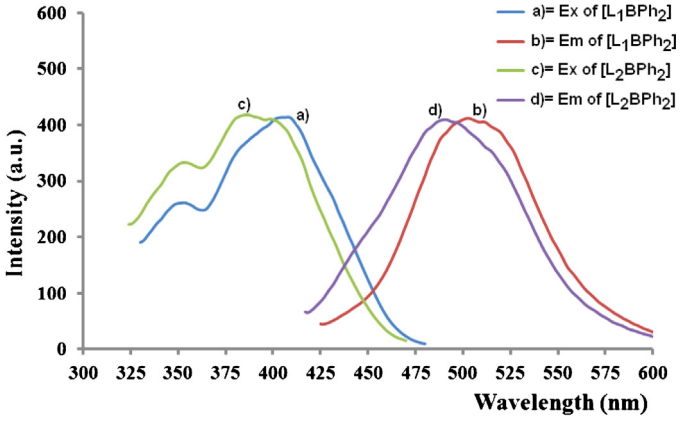

Fig. 3. The fluorescence spectra of $[\mathbf{L_{(1,2)}BPh_2}]$ boron complexes recorded in THF.

due to energy loss via fast rotation of different groups in the salan ($\mathbf{L_2}$) ligand. The emission spectra of boron $[\mathbf{L_{(1,2)}BF_2}]$ and $[\mathbf{L_{(1,2)}BPh_2}]$ complexes are significantly red-shifted in comparison with the free salen ($\mathbf{L_1}$) and salan ($\mathbf{L_2}$) ligands (Figs. 2 and 3). The fluorescence efficiencies of BF_2–chelate boron complexes are greatly improved compared to those of the BPh_2-chelate boron analogs based on the same salen/salan ligands, probably due to the enhanced conjugation degree and of the diphenyl boron chelation, which can effectively prevent molecular aggregation. The difference of fluorescence properties between the salen ($\mathbf{L_1}$) and salan ($\mathbf{L_2}$) ligands and theirfluorine/phenyl boron $[\mathbf{L_{(1,2)}BF_2}]$ and $[\mathbf{L_{(1,2)}BPh_2}]$ complexes may be caused by an increase in rigidity of the salen/salan ligands skeleton of boron complexes due to the chelation of the BF_2 or BPh_2 groups [42]. As shown in Figs. 2 and 3, the fluorescence emission band was observed at 453–503 nm and when excited at 350–385 nm for the complexes, which can be assigned as $\pi \rightarrow \pi^*$ transition, also this bathochromic shift should be due to enlargement of the π system, as a result of p–π conjugation. The formation of the B ← N dative bond via the donation of lone-pair of the N atom to the B atom lowers the energy gap between π^* and π of the free salen ($\mathbf{L_1}$) and salan ($\mathbf{L_2}$) ligands, and the chelating ring makes the ligands more rigid, which can reduce the loss of energy via vibrational motions and increase the emission efficiency [43].

The LC–MS spectra of the free salen ($\mathbf{L_1}$) and salan ($\mathbf{L_2}$) ligands and their fluorine/phenyl boron $[\mathbf{L_{(1,2)}BF_2}]$ and $[\mathbf{L_{(1,2)}BPh_2}]$ complexes were taken as evidence for the formation of the proposed structures. The molecular ion peak is in good agreement with the suggested molecular formula found from elemental analyses and the other spectroscopic methods. The molecular ion peak at m/z = 373.30 (calculated mass: 373.59) amu $[M]^+$ confirms the proposed formula for ligand ($\mathbf{L_1}$), at m/z = 375.32 (calculated mass: 375.60) amu $[M]^+$ confirms the proposed formula for ligand ($\mathbf{L_2}$), at m/z = 420.12 (calculated mass: 420.39) amu $[M]^+$ confirms the proposed formula for $[\mathbf{L_1BF_2}]$, at m/z = 422.32 (calculated mass: 422.40) amu $[M]^+$ confirms the proposed formula for $[\mathbf{L_2BF_2}]$, at m/z = 537.46 (calculated mass: 537.61) amu $[M+H]^+$ confirms the proposed formula for $[\mathbf{L_1BPh_2}]$, and at m/z = 538.43 (calculated mass: 538.62) amu $[M]^+$ confirms the proposed formula for $[\mathbf{L_2BPh_2}]$.

2.3. Catalytic studies

Here, we observe the catalytic activity of boron $[\mathbf{L_{(1,2)}BF_2}]$ and $[\mathbf{L_{(1,2)}BPh_2}]$ complexes in the transfer hydrogenation of aromatic ketones to the corresponding alcohols. In a typical experiment, 0.005 mmol of the complex and 0.5 mmol of ketone were added to a solution of NaOH in *iso*-PrOH (0.025 mmol of NaOH in 5 mL *iso*-PrOH) and refluxed at 82 °C, the reaction being monitored by GC techniques. In all the reactions, fluorine/phenyl boron $[\mathbf{L_{(1,2)}BF_2}]$ and $[\mathbf{L_{(1,2)}BPh_2}]$ complexes catalyzed the reduction of ketones to the corresponding alcohols via hydrogen transfer from *iso*-PrOH.

Recently, we have reported that the fluorine/phenyl boron complexes as active catalysts in the reduction of aromatic ketones [21]. The observed activity of these fluorine/phenyl boron complexes have encouraged us to investigated other analogous ligands. These fluorine/phenyl boron $[\mathbf{L_{(1,2)}BF_2}]$ and $[\mathbf{L_{(1,2)}BPh_2}]$ complexes as catalyst precursors for the transfer hydrogenation of acetophenone have been tested and typical results are summarized in Table 1. As seen Table 1, with a complex/NaOH ratio of 1/5, the complexes are very active leading to a quantitative transformation of the acetophenone. At room temperature no noticeable formation of 1-phenylethanol was observed (Table 1, entries 1–4). Furthemore, as can be inferred from Table 1 (entries 5–8), the precatalysts as well as the presence of NaOH are necessary to observe appreciable conversions. The base facilitates the formation of boron alkoxide by abstracting proton of the alcohol and subsequently alkoxide undergoes β-elimination to give hydride, which is an active species in this reaction. The role of the base is to generate a more nucleophilic alkoxide ion which would rapidly attack the boron complex responsible for dehydrogenation of *iso*-PrOH. As Table 1 shows, high conversions can be achieved with the $[\mathbf{L_{(1-2)}BF_2}]$ and $[\mathbf{L_{(1-2)}BPh_2}]$ catalytic systems. The results of optimization studies showed clearly that the excellent conversions were achieved in the reduction of acetophenone to 1-phenylethanol when the complex $[\mathbf{L_2BPh_2}]$ was used as the catalytic

Table 1
Transfer hydrogenation of acetophenone with *iso*-PrOH catalyzed by [$\mathbf{L_1BF_2}$], [$\mathbf{L_1BPh_2}$], [$\mathbf{L_2BF_2}$] and [$\mathbf{L_2BPh_2}$].

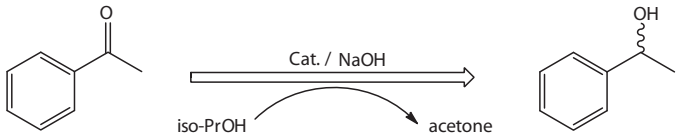

Entry	Catalyst	S/C/NaOH	Time	Conversion (%)[d]	TOF (h^{-1})[e]
1	[$\mathbf{L_1BF_2}$][a]	100:1:5	48 h	Trace	–
2	[$\mathbf{L_1BPh_2}$][a]	100:1:5	48 h	Trace	–
3	[$\mathbf{L_2BF_2}$][a]	100:1:5	48 h	Trace	–
4	[$\mathbf{L_2BPh_2}$][a]	100:1:5	48 h	Trace	–
5	[$\mathbf{L_1BF_2}$][b]	100:1	48 h	<3	–
6	[$\mathbf{L_1BPh_2}$][b]	100:1	48 h	<3	–
7	[$\mathbf{L_2BF_2}$][b]	100:1	48 h	<3	–
8	[$\mathbf{L_2BPh_2}$][b]	100:1	48 h	<3	–
9	[$\mathbf{L_1BF_2}$][c]	100:1:5	12 h	98	<10
10	[$\mathbf{L_1BPh_2}$][c]	100:1:5	15 h	99	<10
11	[$\mathbf{L_2BF_2}$][c]	100:1:5	15 h	99	<10
12	[$\mathbf{L_2BPh_2}$][c]	100:1:5	8 h	99	12

Reaction conditions:
[a] At room temperature; acetophenone/Cat./NaOH, 100:1:5.
[b] Refluxing in *iso*-PrOH; acetophenone/Cat, 100:1, in the absence of base.
[c] Refluxing in *iso*-PrOH; acetophenone/Cat/NaOH, 100:1:5.
[d] Determined by GC (three independent catalytic experiments).
[e] Referred at the reaction time indicated in column; TOF = (mol product/mol Cat.) × h^{-1}.

precursor, with a substrate-catalyst molar ratio (100:1) in *iso*-PrOH at 82 °C (Table 1, entries 9–12).

Encouraged by the high catalytic activities gained in these preliminary studies, we next extended our investigations to include hydrogenation of acetophenone derivatives. A variety of simple ketones (S/C = 100/1) can be transformed to the corresponding secondary alcohols with high conversion, as exemplified in Table 2. The complexes [$\mathbf{L_1BF_2}$] and [$\mathbf{L_2BPh_2}$] were also extensively investigated with a variety of substrates. As expected, electronic properties (the nature and position) of the substituents on the phenyl ring of the ketone caused the changes in the reduction degree. To ensure that the observed results could be attributed to purely electronic effects [44], substrates involving *para*- and *ortho*-substituted acetophenone derivatives were investigated. The results indicated that a strong electron withdrawing substituents, such as F, Cl and Br were capable of higher conversion (Table 2). Conversely, the most electron-donor substituents, (2-methoxy or 4-methoxy) led to lower conversion. It is well-known that the presence of an electron withdrawing group has generally been found to facilitate the hydrogen transfer reaction [45,46], and this has been attributed to the hydridic nature of the reducing species involved. As such, reactions with fluoro proceeded to higher conversion owing to rapid hydride transfer, while reactions with electron-donating substituents

Table 2
Transfer hydrogenation results for substituted acetophenones with the catalyst system, [$\mathbf{L_1BF_2}$] and [$\mathbf{L_2BPh_2}$].[a]

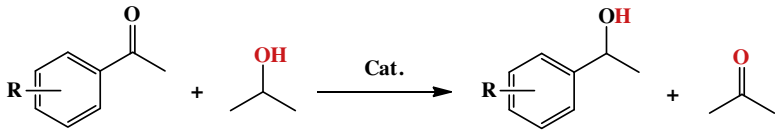

Entry	R	Time	Conversion (%)[b]	TOF (h^{-1})[c]
Cat: [$\mathbf{L_1BF_2}$]				
1	4-F	9 h	99	10
2	4-Cl	10 h	98	10
3	4-Br	12 h	99	<10
4	4-NO_2	8 h	98	12
5	4-Me	18 h	99	<10
6	4-MeO	20 h	98	<10
Cat: [$\mathbf{L_2BPh_2}$]				
1	4-F	6 h	99	17
2	4-Cl	8 h	98	12
3	4-Br	9 h	99	11
4	4-NO_2	5 h	98	20
5	4-Me	12 h	99	<10
6	4-MeO	15 h	98	<10

Reaction conditions:
[a] Catalyst (0.005 mmol), substrate (0.5 mmol), *iso*-PrOH (5 mL), NaOH (0.025 mmol %), 82 °C, respectively, the concentration of acetophenone derivatives is 0.1 M.
[b] Purity of compounds is checked by NMR and GC (three independent catalytic experiments), yields are based on methyl aryl ketone.
[c] TOF = (mol product/mol Cat.) × h^{-1}.

(2-methoxy or 4-methoxy) proceeded in a slower and more controlled manner [22,47]. The examination of the results indicates clearly that with each of the tested complexes, the best yield was achieved in the reduction of acetophenone derivatives when [$\mathbf{L_2BPh_2}$] was used as the catalyst precursor.

3. Conclusion

In summary, we have isolated and structurally characterized two ligands and their fluorine/phenyl boron [$\mathbf{L_{(1,2)}BF_2}$] and [$\mathbf{L_{(1,2)}BPh_2}$] complexes. The absorption spectra, NMR spectra, FT-IR spectra, LC–MS spectra and fluorescence properties of the boron [$\mathbf{L_{(1,2)}BF_2}$] and [$\mathbf{L_{(1,2)}BPh_2}$] complexes have been thoroughly investigated and compared with those of free salen ($\mathbf{L_1}$) and salan ($\mathbf{L_2}$) ligands. The fluorescence efficiencies of BF_2–chelate boron complexes are greatly improved compared to those of the BPh_2-chelate boron analogs based on the same salen/salan ligands, probably due to the enhanced conjugation degree and of the diphenyl boron chelation, which can effectively prevent molecular aggregation. Furhermore, these fluorine/phenyl boron [$\mathbf{L_{(1,2)}BF_2}$] and [$\mathbf{L_{(1,2)}BPh_2}$] complexes catalyzed the reduction of acetophenone derivatives via hydrogen transfer from *iso*-PrOH. They have also exhibited promising catalytic activity in the transfer hydrogenation reaction of various ketones. The procedure is simple and efficient towards various aryl ketones. Future investigations are aiming at the development of an asymmetric version of this process.

4. Experimental

4.1. Materials and measurements

All reagents and solvents were of reagent-grade and obtained from commercial suppliers. ^{1}H and ^{13}C NMR with ^{19}F NMR spectra were recorded at 25 °C using a Agilent-VNMRS-400 spectrometer operating at 400.1 MHz, 100.6 MHz, and 376.3 MHz, respectively. Infrared spectra were recorded on a Perkin Elmer Spectrum RXI FT-IR spectrometer (4000–400 cm^{-1}) as KBr pellets. Elemental analyses were performed by using a LECO CHNS model 932 elemental analyzer. UV–vis spectra were obtained with a Perkin-Elmer model Lambda 25 spectrophotometer in the wavelength range from 200 to 1100 nm at room temperature. Fluorescence spectra were obtained with Perkin-Elmer model LS55 spectrometer. Melting points were measured in open capillary tubes with an Electrothermal 9100 melting point apparatus and are uncorrected. LC–MS results were recorded on an Agilent LC/MSD LC–MS/MS spectrometer. GC analyses were performed on a Shimadzu 2010 Plus HP 6890N Gas Chromatograph.

4.2. General procedure for the transfer hydrogenation of ketones

Typical procedure for the catalytic hydrogen-transfer reaction: a solution of the boron complexes [$\mathbf{L_{(1\text{-}2)}BF_2}$] as electron donors and phenyl boron complexes [$\mathbf{L_{(1\text{-}2)}BPh_2}$] as electron acceptors (0.005 mmol), NaOH (0.025 mmol) and the corresponding ketone (0.5 mmol) in degassed *iso*-PrOH (5 mL) were refluxed until the reactions were completed. Then, an aliquot of the catalytic solution (1 mL) was removed with a syringe and evaporated under reduced pressure. The resultant oil was subjected to flash chromatography (silica gel-60, Et_2O) and subsequently evaporated under reduced pressure to yield clear liquids in each case. After this time, a sample of the reaction mixture is taken off, diluted with acetone and analyzed immediately by GC. Conversions obtained are related to the residual unreacted ketone. Furthermore, ^{1}H NMR spectral data for the resultant products were consistent with previously reported results.

4.3. GC analysis

GC analyses were performed on a Shimadzu 2010 Plus HP 6890N Gas Chromatograph equipped with capillary column (5% biphenyl, 95% dimethylsiloxane) (30 m × 0.32 mm × 0.25 μm). The GC parameters were for transfer hydrogenation of ketones as follows; initial temperature, 110 °C; initial time, 1 min; solvent delay, 4.48 min; temperature ramp 80 °C/min; final temperature, 200 °C; final time, 21.13 min; injector port temperature, 200 °C; detector temperature, 200 °C, injection volume, 2.0 μL.

4.4. Synthesis of the ligands

4.4.1. Synthesis of the ligand (L_1)

The salen ligand ($\mathbf{L_1}$) was synthesized by a reported procedure with some modifications [48]. Color: yellow, yield: 86%, m.p: 115 °C. Anal. Calc. for [$C_{24}H_{40}N_2O$] (mw: 372.6 g/mol): C, 77.37; H, 10.82; N, 7.52, found: C, 77.01; H, 10.96; N, 7.44; LC–MS (Scan ES$^+$): *m*/*z* (%) calculated mass [M+H]$^+$: 373.59, found: 373.30 (1 0 0). FT-IR (KBr pellets, υ_{max}/cm^{-1}): 3258 υ(NH), 3182–2643 υ(O–H···N), 3060 υ(Ar–CH), 2956–2871 υ(Aliph-CH), 1632 υ(C=N) and 1174 υ(C–O); ^{1}H NMR ($CDCl_3$, TMS, 400.1 MHz, δ ppm): 13.91 (s, 1H, O<u>H</u>), 8.49 (s, 1H, <u>H</u>C=N), 7.39 (d, 1H, Ar–C<u>H</u>), 7.13 (d, 1H, Ar–C<u>H</u>), 4.01 (d, 1H, C<u>H</u>–CH_2), 2.35 (d, 2H, CH–C<u>H</u>$_2$), 2.11 (d, 2H, CH–C<u>H</u>$_2$), 1.86 (s, 1H, N<u>H</u>) and 1.80–1.52 (m, 30H, C–C<u>H</u>$_3$); ^{13}C NMR ($CDCl_3$, TMS, 100.6 MHz, δ ppm): 164.54 (H<u>C</u>=N), 158.40, 140.33, 137.03, 127.11, 126.13, 118.24 (Ar–<u>C</u>H), 61.42 (<u>C</u>–CH_3), 51.41 (CH–<u>C</u>H$_2$), 46.38 (<u>C</u>H–CH_2), 35.38 (<u>C</u>–CH_3), 34.94 (C–<u>C</u>H$_3$), 31.87 (C–<u>C</u>H$_3$) and 28.71 (C–<u>C</u>H$_3$); UV–vis (λ_{max}, nm): 233, 259, and 329 (CH_3OH); 227, 262 and 328 (THF).

4.4.2. Synthesis of the ligand (L_2)

To a stirred solution of ligand ($\mathbf{L_1}$) (1.50 g, 4.03 mmol) in absolute ethanol (70 mL), sodium borohydride (0.98 g, 24.17 mmol) was slowly added at 0 °C temperature. When the mixture was colorless at room temperature for 24 h, it was poured over distilled water (70 mL) and extracted with dichloromethane. The combined organic phases were dried and the solvents were removed in vacuo. The white solid of salan ligand ($\mathbf{L_2}$) was obtained from recrystallization in a mixture of chloroform ($CHCl_3$) and CH_3OH. Color: white, yield: 78%, m.p: 182 °C. Anal. Calc. for [$C_{24}H_{42}N_2O$] (mw: 374.6 g/mol): C, 76.95; H, 11.30; N, 7.48; found: C, 76.83; H, 11.24; N, 7.53. LC–MS (Scan ES$^+$): *m*/*z* (%) calculated mass [M+H]$^+$: 375.60, found: 375.32 (100). FT-IR (KBr pellets, υ_{max}/cm^{-1}): 3275 υ(NH), 3117–2640 υ(O–H···N), 3000 υ(Ar–CH), 2955–2865 υ(Aliph–CH), 1606 υ(NH) and 1166 υ(C–O); ^{1}H NMR ($CDCl_3$, TMS, 400.1 MHz, δ ppm): 13.82 (s, 1H, O<u>H</u>), 7.17 (d, 1H, Ar–C<u>H</u>), 6.83 (d, 1H, Ar–C<u>H</u>), 4.03 (s, 2H, NH–C<u>H</u>$_2$), 3.94 (t, 1H, C<u>H</u>–CH_2), 2.98 (s, 2H, N<u>H</u>), 1.92 (d, 4H, CH–C<u>H</u>$_2$) and 1.39–1.08 (m, 30H, C–C<u>H</u>$_3$); ^{13}C NMR ($CDCl_3$, TMS, 100.6 MHz, δ ppm): 154.92, 140.80, 136.36, 123.38, 123.21, 122.86 (Ar–<u>C</u>H), 51.36 (<u>C</u>–CH_3), 50.70 (<u>C</u>H–CH_2), 49.90 (CH–<u>C</u>H$_2$), 46.09 (<u>C</u>H$_2$–NH), 35.38 (<u>C</u>–CH_3), 35.21 (C–<u>C</u>H$_3$), 31.98 (C–<u>C</u>H$_3$), 29.94 (C–<u>C</u>H$_3$). and 29.00 (C–<u>C</u>H$_3$); UV–vis (λ_{max}, nm, * = shoulder peak): 232* and 283 (CH_3OH); 226, 282 and 335* (THF).

4.5. Synthesis of the BF_2-chelated boron complexes [$L_{(1,2)}BF_2$]

In a two-necked, 100 mL round-bottom flask and equipped with a blanket of nitrogen (N_2) was placed 40 mL of anhydrous benzene at room temperature. To this solution it was added 0.50 g, 1.34 mmol of ligand ($\mathbf{L_1}$) and 0.50 g, 1.33 mmol of ligand ($\mathbf{L_2}$) in 15 mL anhydrous benzene respectively, followed by triethylamine (Et_3N) (0.2 mL, 1.34 mmol) was added to the for each solution. After the reaction mixture was stirred for 50 min, boron trifluoride diethyl etherate ($BF_3{\cdot}Et_2O$) (0.50 mL, 4.02 mmol) was added

slowly. The mixture was stirred at 40 °C for 14 h and then yellowish compound for [$\mathbf{L_1BF_2}$] or white compound for [$\mathbf{L_2BF_2}$] was gradually precipitated from the solution. After cooling to room temperature, the solution was filtrated and the product was washed several times with hexane and diethyl ether, successively. The solid product was then purified by recrystallization and sublimation.

4.5.1. Synthesis of the complex [L_1BF_2]

Color: yellow, yield: 72%, m.p: 162 °C. Anal. Calc. for [$C_{24}H_{39}N_2OBF_2$] (mw: 420.4 g/mol): C, 68.57; H, 9.35; N, 6.66; found: C, 68.49; H, 9.39; N, 6.59; LC–MS (Scan ES$^+$): *m/z* (%) calculated mass [M]$^+$: 420.39, found: 420.12 (35). FT-IR (KBr pellets, υ_{max}/cm^{-1}): 3195 υ(N–H), 3129 υ(Ar–CH), 2969–2847 υ(Aliph-CH), 1623 υ(C=N), 1183 υ(B–O), 1165 υ(C–O), 1060 υ(B–N) and 882 υ(B–F); ^{1}H NMR ($CDCl_3$, TMS, 400.1 MHz, δ ppm): 8.38 (s, 1H, HC=N), 7.79 (d, 1H, Ar–CH), 7.61 (d, 1H, Ar–CH), 4.40–4.36 (m, 1H, CH–CH_2), 2.28 (d, 2H, CH–CH_2), 2.14 (d, 2H, CH–CH_2), 1.88 (s, 1H, NH) and 1.99–1.85 (m, 30H, C–CH_3); ^{13}C NMR ($CDCl_3$, TMS, 100.6 MHz, δ ppm): 163.32 (HC=N), 153.35, 135.98, 131.79, 122.64, 122.54, 113.78 (Ar–CH), 66.72 (C–CH_3), 53.05 (CH–CH_2), 52.39 (CH–CH_2), 41.88 (C–CH_3), 38.11 (C–CH_3), 30.66 (C–CH_3), 29.98 (C–CH_3), 27.38 (C–CH_3) and 26.16 (C–CH_3); ^{19}F NMR (DMSO-d_6, 376.3 MHz, δ ppm) −148.35 (q, $J_{(B-F)}$ = 31 Hz, BF_2). UV–vis (λ_{max}, nm, * = shoulder peak): 223, 262, 292* and 332 (CH_3OH); 227, 261, 286* and 329 (THF).

4.5.2. Synthesis of the complex [L_2BF_2]

Color: white, yield: 68%, m.p: 145 °C. Anal. Calc. for [$C_{24}H_{41}N_2OBF_2$] (mw: 422.4 g/mol): C, 68.24; H, 9.78; N, 6.63; found: C, 68.18; H, 9.70; N, 6.67; LC–MS (Scan ES$^+$): *m/z* (%) calculated mass [M]$^+$: 422.40, found: 422.32 (25). FT-IR (KBr pellets, υ_{max}/cm^{-1}): 3169 υ(N–H), 3095 υ(Ar–CH), 2969–2878 υ(Aliph-CH) 1578 υ(N–H), 1186 υ(B–O), 1167 υ(C–O), 1057 υ(B–N) and 876 υ(B–F); ^{1}H NMR ($CDCl_3$, TMS, 400.1 MHz, δ ppm): 7.70 (d, 1H, Ar–CH,), 7.36 (d, 1H, Ar–CH,), 4.50 (d, 2H, NH–CH_2,), 3.68 (s, 1H, CH–CH_2), 1.99 (s, 2H, NH), 1.84 (d, 4H, CH–CH_2) and 1.40–1.04 (m, 30H, C–CH_3); ^{13}C NMR ($CDCl_3$, TMS, 100.6 MHz, δ ppm): 154.64, 143.32, 133.78, 129.80, 124.21, 121.18, 114.46 (Ar–CH), 59.24 (C–CH_3), 50.48 (CH–CH_2), 47.66 (CH–CH_2), 47.61 (CH_2–NH), 41.33 (C–CH_3), 35.46 (C–CH_3), 32.22 (C–CH_3), 30.75 (C–CH_3). and 25.39 (C–CH_3); ^{19}F NMR (DMSO-d_6, 376.3 MHz, δ ppm) −148.44 (q, $J_{(B-F)}$ = 30 Hz, BF_2). UV–vis (λ_{max}, nm, * = shoulder peak): 220*, 281 and 348* (CH_3OH); 245, 265, 290 and 352 (THF).

4.6. Synthesis of the BPh_2-chelated boron complexes [$L_{(1,2)}BPh_2$]

In a two-necked, 100 mL round-bottom flask and equipped with a blanket of nitrogen (N_2) was placed 20 mL of anhydrous toluene. To this solution it was added 0.50 g, 1.34 mmol for ligand ($\mathbf{L_1}$) and 0.50 g, 1.33 mmol for ligand ($\mathbf{L_2}$) in 20 mL anhydrous toluene, respectively. After the reaction mixture was stirred for 60 min at room temperature, followed by triphenyl borane (BPh_3) (0.48 g, 2.01 mmol) was added slowly into this solution and the mixture was stirred at reflux temperature for 18 h and light yellow compound of [$\mathbf{L_1BPh_2}$] and white compound of [$\mathbf{L_2BPh_2}$] were gradually precipitated from the solution. After cooling to room temperature, the solution was filtrated and the products were washed several times by hexane and diethyl ether, successively. The solid product was purified by recrystallization in a mixture of $CHCl_3$/hexane.

4.6.1. Synthesis of the complex [L_1BPh_2]

Color: light yellow, yield: 70%, m.p: 108 °C; Anal. Calc. for [$C_{24}H_{39}N_2OBPh_2$] (mw: 536.6 g/mol): C, 80.58; H, 9.20; N, 5.22; found: C, 80.51; H, 9.28; N, 5.16; LC–MS (Scan ES$^+$): *m/z* (%) calculated mass [M+H]$^+$: 537.61, found: 537.46 (30). FT-IR (KBr pellets, υ_{max}/cm^{-1}): 3068 υ(Ar–CH), 2956–2847 υ(Aliph-CH), 1620 υ(C=N), 1602 υ(N–H), 1190 υ(B–O), 1156 υ(C–O), 1028 υ(B–N) and 886 υ(B–Ph); ^{1}H NMR ($CDCl_3$, TMS, 400.1 MHz, δ ppm): 8.31 (s, 1H, HC=N), 7.79 (d, 4H, Ph–CH,), 7.73 (d, 1H, Ar–CH), 7.68 (d, 1H, Ar–CH), 7.45–7.32 (m, 6H, Ph–CH), 3.78–3.363 (m, 1H, CH–CH_2), 2.02 (s, 1H, NH), 1.62 (d, 4H, CH–CH_2) 1.47 (s, 18H, C–CH_3) and 1.34 (s, 12H, C–CH_3); ^{13}C NMR (DMSO-d_6, TMS, 100.6 MHz, δ ppm): 160.93 (HC=N), 144.72, 140.08, 139.91, 137.96, 137.63, 135.11, 134.12, 134.01, 132.77, 131.85, 131.42, 126.49, 125.70, 119.41 and 113.27 (Ar–CH), 54.08 (C–CH_3), 51.94 (CH–CH_2), 45.56 (CH_2–NH), 37.85 (C–CH_3), 34.91 (C–CH_3), 31.55 (C–CH_3), 29.80 (C–CH_3). and 28.05 (C–CH_3). UV–vis (λ_{max}, nm): 243, 292 and 392 (CH_3OH); 248, 267, 292 and 391 (THF).

4.6.2. Synthesis of the complex [L_2BPh_2]

Color: white, yield: 65%, m.p: 119 °C; Anal. Calc. for [$C_{24}H_{41}N_2OBPh_2$] (mw: 538.6 g/mol): C, 80.28; H, 9.54; N, 5.20; found: C, 80.23; H, 9.58; N, 5.18; LC–MS (Scan ES$^+$): *m/z* (%) calculated mass [M]$^+$: 538.62, found: 538.43 (42). FT-IR (KBr pellets, υ_{max}/cm^{-1}): 3051 and 3026 υ(Ar–CH), 2964–2871 υ(Aliph-CH) 1608 υ(N–H), 1183 υ(B–O), 1166 υ(C–O), 1017 υ(B–N) and 882 υ(B–Ph); ^{1}H NMR ($CDCl_3$, TMS, 400.1 MHz, δ ppm): 7.76 (d, 1H, Ar–CH), 7.68 (d, 1H, Ar–CH), 7.43–7.25 (m, 10H, Ph–CH), 4.26 (s, 2H, NH–CH_2), 3.24 (s, 1H, CH–CH_2), 2.71 (s, 2H, NH), 1.89 (d, 4H, CH–CH_2) and 1.38–1.02 (m, 30H, C–CH_3); ^{13}C NMR ($CDCl_3$, TMS, 100.6 MHz, δ ppm): 154.68, 140.23, 140.01, 138.07, 137.61, 134.92, 134.20, 133.86, 132.68, 132.15, 131.73, 126.32, 126.04, 119.30 and 114.38 (Ar–CH), 56.12 (C–CH_3), 52.46 (CH–CH_2), 46.73 (CH_2–NH), 37.82 (C–CH_3), 35.23 (C–CH_3), 32.17 (C–CH_3), 28.93 (C–CH_3). and 28.12 (C–CH_3); UV–vis (λ_{max}, nm, * = shoulder peak): 236, 251, 337 and 402* (CH_3OH); 248, 291, 332 and 398* (THF).

Acknowledgements

Partial support from Harran University (HUBAK Project No: 12159, Sanliurfa, Turkey), Dicle University (Project number: 2009 DPTK 120580) and Science and Technology Application and Research Center (DÜPTAM) is gratefully acknowledged.

References

[1] A.C. Benniston, G. Copley, Phys. Chem. 11 (2009) 4124–4131.
[2] R. Ziessel, G. Ulricha, A. Harrimanb, New J. Chem. 31 (2007) 496–501.
[3] Q.C. Yao, D.E. Wu, R.Z. Ma, M. Xia, J. Organomet. Chem. 743 (2013) 1–9.
[4] C. McDonagh, C.S. Burke, B.D. MacCraith, Chem. Rev. 108 (2008) 400–422.
[5] Z.C. Xu, J. Yoon, D.R. Spring, Chem. Soc. Rev. 39 (2010) 1996–2006.
[6] X. Liu, Y. Ren, H. Xia, X. Fan, Y. Mu, Inorg. Chim. Acta 363 (2010) 1441–1447.
[7] A. Coskun, E.U. Akkaya, J. Am. Chem. Soc. 127 (2005) 10464–10465.
[8] K. Yamada, Y. Nomura, D. Citterio, N. Iwasawa, K. Suzuki, J. Am. Chem. Soc. 127 (2005) 6956–6957.
[9] X. Zhang, H.S. Zhang, Spectrochim. Acta A 61 (2005) 1045–1049.
[10] R. Guliyev, O. Buyukcakir, F. Sozmen, O.A. Bozdemir, Tetrahedron Lett. 50 (2009) 5139–5141.
[11] R.C. Evans, P. Douglas, C.J. Winscom, Coord. Chem. Rev. 250 (2006) 2093.
[12] G.E. Morse, T.P. Bender, ACS Appl. Mater. Interfaces 4 (2012) 5055–5068.
[13] C.D. Entwistle, T.B. Marder, Chem. Mater. 16 (2004) 4574–4585.
[14] Y. Li, Y. Liu, W. Bu, J. Guo, Y. Wang, Chem. Commun. 16 (2000) 1551–1552.
[15] S. Ertan-Ela, M.D. Yilmaz, B. Icli, Y. Dede, S. Icli, E.U. Akkaya, Org. Lett. 10 (2008) 3299–3302.
[16] T. Rousseau, A. Cravino, T. Bura, G. Ulrich, R. Ziessel, J. Roncali, Chem. Commun. 13 (2009) 1673–1675.
[17] D. Liu, M. Mudadu, R. Thummel, Y. Tao, S. Wang, Adv. Funct. Mater. 15 (2005) 143–154.
[18] Z.Q. Liu, Q. Fang, D. Wang, G. Xue, W.T. Yu, Z.S. Shao, M.H. Jing, Chem. Commun. 23 (2002) 2900–2901.
[19] D.O. Frimannsson, M. Grossi, J. Murtagh, F. Paradisi, D.F. O'Shea, J. Med. Chem. 53 (2010) 7337–7343.
[20] P. Pelagatti, M. Carcelli, F. Calbiani, C. Cassi, L. Elviri, C. Pelizzi, U. Rizzotti, D. Rogolino, Organometallics 24 (2005) 5836–5844.
[21] A. Kilic, C. Kayan, M. Aydemir, F. Durap, M. Durgun, A. Baysal, E. Tas, B. Gumgum, Appl. Organomet. Chem. 25 (2011) 390–394.
[22] J.W. Faller, A.R. Lavoie, Organometallics 20 (2001) 5245–5247.

[23] Q.D. Liu, M.S. Mudadu, R. Thummel, Y. Tao, S. Wang, Adv. Funct. Mater. 15 (2005) 143–154.
[24] Q. Hou, L. Zhao, H. Zhang, Y. Wang, S. Jiang, J. Lumin. 126 (2007) 447–451.
[25] E.A. Braude, R.P. Linstead, J. Chem. Soc. (1954) 3544–3547.
[26] E. Marza, M. Sanau, E. Peris, Inorg. Chem. 44 (2005) 9961–9967.
[27] M.J. Albrecht, R. Miecznikowski, A. Samuel, J.W. Faller, R.H. Crabtree, Organometallics 21 (2002) 3596–3604.
[28] R.A.W. Johnstone, A.H. Wilby, I.D. Entwistle, Chem. Rev. 85 (1985) 129.
[29] M. Yiğit, B. Yiğit, I. Özdemir, E. Çetinkaya, B. Çetinkaya, Appl. Organomett. Chem. 20 (2006) 322.
[30] R. Noyori, M. Yamakawa, S. Hashiguchi, Acc. Chem. Res. 23 (1990) 345.
[31] S. Ram, R.E. Ehrenkaufer, Synthesis 2 (1998) 91–95.
[32] O. Pamies, J.E. Backvall, Chem. Eur. J. 23 (2001) 5052.
[33] H. Meerwein, R. Schmidt, J. Liebigs, Ann. Chem. 444 (1925) 221.
[34] A. Verley, Bull. Soc. Fr. 37 (1925) 537.
[35] W. Ponndorf, Angew. Chem. 39 (1926) 138.
[36] J. Trocha-Grihmshaw, H.B. Henbest, Chem. Commun. (1967) 544.
[37] T. Kariya, A.J. Blacker, Acc. Chem. Res. 40 (2007) 1300–1308.
[38] P. Sharma, V. Vajpayee, J. Sharma, Y. Singh, Appl Organomett. Chem. 24 (2010) 774–780.
[39] D.J. Wang, B.P. Xu, X.H. Wei, J. Zheng, J. Fluorine Chem. 140 (2012) 49–53.
[40] N.M.D. Brown, P. Bladon, J. Chem. Soc. A (1969) 526–532.
[41] H.H. Zhang, X. Hu, W. Dou, W.S. Liu, J. Fluorine Chem. 131 (2010) 883–887.
[42] R.Z. Ma, Q.C. Yao, X. Yang, M. Xia, J. Fluorine Chem. 137 (2012) 93–98.
[43] Y. Ren, X. Liu, W. Gao, H. Xia, L. Ye, Y. Mu, Eur. J. Inorg. Chem. 13 (2007) 1808–1814.
[44] T.H. Lowry, K.S. Richardson, Mechanism and Theory in Organic Chemistry, Harper Collins, New York, 1987 (Chapter 2).
[45] I. Yamada, R. Noyori, Org. Lett. 2 (2000) 3425–3427.
[46] M.J. Palmer, M. Wills, Tetrahedron: Asymm. 10 (1999) 2045–2061.
[47] D.H. McDaniel, H.C. Brown, J. Org. Chem. 23 (1958) 420–427.
[48] E. Tas, I. Ucar, V.T. Kasumov, A. Kilic, A. Bulut, Spectrochim. Acta A 68 (2007) 463–468.